



Gain and index guiding effects in an injection seeded Raman amplifier
by Kevin Scot Repasky

A thesis submitted in partial fulfillment of the requirements for the degree of Doctor of Philosophy in
Physics

Montana State University

© Copyright by Kevin Scot Repasky (1996)

Abstract:

A theory is presented for an injection seeded Raman amplifier which includes the total Raman susceptibility. Calculations indicate that the imaginary part of the Raman susceptibility leads to gain and gain guiding while the real part of the Raman susceptibility leads to index guiding. Both the gain and index guiding affect the spatial structure of the amplified Stokes beam. When the input Stokes beam is tuned to the blue (red) side of the Raman resonance, the amplified Stokes beam is focused (defocused) due to the real part of the Raman susceptibility. The calculations also indicate the peak Stokes output from the Raman amplifier occurs when the input Stokes is tuned to the blue side of the Raman resonance. Experimental results are presented that measure the amplified Stokes beam's spatial structure. The results from this experiment confirm the prediction of a narrower (wider) Stokes beam when the input Stokes is tuned to the blue (red) side of the Raman resonance. The narrower amplified Stokes beam when the input Stokes is tuned to the blue side of the Raman resonance results in the amplified Stokes beam experiencing an increased gain. This increased gain that occurs on the blue side of the Raman resonance is confirmed by an experiment.

GAIN AND INDEX GUIDING EFFECTS IN AN INJECTION SEEDED RAMAN
AMPLIFIER

by

Kevin Scot Repasky

A thesis submitted in partial fulfillment
of the requirements for the degree

of

Doctor of Philosophy

in

Physics

MONTANA STATE UNIVERSITY
Bozeman, Montana

December 1996

D378
R299

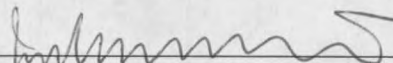
APPROVAL

of a thesis submitted by

Kevin Scot Repasky

This thesis has been read by each member of the thesis committee and has been found to be satisfactory regarding content, English usage, format, citations, bibliographic style, and consistency, and is ready for submission to the College of Graduate Studies.

John L. Carlsten

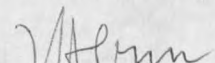


Chairperson, Graduate Committee

1-13-97
Date

Approved for the Department of Physics

John Hermanson

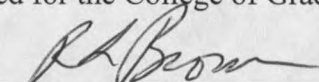


Head, Major Department

1-13-97
Date

Approved for the College of Graduate Studies

Graduate Dean



1/20/97
Date

STATEMENT OF PERMISSION TO USE

In presenting this thesis in partial fulfillment of the requirements for a doctoral degree at Montana State University-Bozeman, I agree that the Library shall make it available to borrowers under rules of the Library. I further agree that copying of this thesis is allowed only for scholarly purposes, consistent with "fair use" as prescribed in the U.S. Copyright Law. Requests for extensive copying or reproduction of this thesis should be referred to University Microfilms International, 300 North Zeeb Road, Ann Arbor, Michigan 48106, to whom I have granted "the exclusive right to reproduce and distribute my dissertation in and from microform along with the non-exclusive right to reproduce and distribute my abstract in any format in whole or in part."

Signature Kevin Repachy

Date 1-13-97

ACKNOWLEDGMENTS

First and foremost, I would like to thank my advisor, John Carlsten, for giving me the opportunity to work in his lab. His infinite patience and encouragement has made my tenure in his lab a most rewarding experience.

I would like to thank the many people who I have had the pleasure to work with. Thanks are due to Jim Wessel who helped me get started in the lab. We had many great times, laughs, and late nights. Also, thanks are due to Jay Brasseur for help on the latest experiments. Also, thanks go to Gregg Switzer, Meg Hall and the numerous undergraduates who have worked in the lab.

I am grateful to my graduate committee for reading my thesis. I have incorporated many of their suggested changes into this thesis.

I would like to thank Erik Anderson and Norm Williams for their help with electronics and machining.

I would like to thank my mom for encouraging me to chase my dreams. Also thanks go to Dr. and Mrs. Ketcham for all their help that I will never be able to repay.

Finally, thanks go to my wife Terry Rick who has supported me throughout.

TABLE OF CONTENTS

	Page
1. INTRODUCTION	1
Raman Scattering	1
Background	3
Gain and Index Guiding	4
2. THE WAVE EQUATION AND METHOD OF SOLUTION	11
Introduction	11
Wave Equation	12
The Nonlinear Raman Susceptibility	13
Approximate Solution to the Wave Equation	14
Solution to the Wave Equation	17
The Gauss-Laguerre Basis	18
The Nonorthogonal Basis	22
3. MODE STRUCTURE OF THE AMPLIFIED STOKES FIELD	27
Introduction	27
Physical Arguments for Gain and Index Guiding	28
Mode Structure of the Amplified Stokes Field	29
Enhanced Performance of a Raman Amplifier	33
4. SEEDING OF A RAMAN AMPLIFIER WITH A VISIBLE LASER DIODE	45
Introduction	45
Experiment	46
High Finesse Interferometers	48
Results	52
5. SPATIAL STRUCTURE OF THE AMPLIFIED STOKES FIELD	60
Introduction	60
Spatial Structure Experiment	61
Results	64
6. FREQUENCY ASYMMETRIC GAIN PROFILE IN A SEEDED RAMAN AMPLIFIER	73
Introduction	73

TABLE OF CONTENTS - Continued

	Frequency Dependence of the Stokes Output	74
	Experiment	77
	Experimental Results	78
7.	CONCLUSION	86
	Summary	86
	Future	88
	REFERENCES CITED	89
	APPENDICES	94
A.	The Wave Equation	95
B.	Transient Stimulated Raman Scattering Equations	98
C.	The Nonlinear Raman Susceptibility	101
D.	The Gauss-Laguerre Modes	107
E.	The $A_{p',p}^l(\mu, G; \theta, \theta_m)$ Matrix Elements	114
F.	Mode Matching and Alignment of the High Finesse Interferometer	117
G.	Raman Linewidth	124

LIST OF FIGURES

Figure	Page
1. Energy level diagram	9
2. Simplified experimental setup	10
3. Gain guiding	36
4. Phasefronts affected by a lens	37
5. Phasefronts for zero detuning	38
6. Spatial profile for zero detuning	39
7. Phasefronts for detuning to the blue side of the Raman resonance	40
8. Phasefronts for detuning to the red side of the Raman resonance	41
9. Spatial profiles including detuning	42
10. Phasefronts including modified input	43
11. Enhanced performance for modified input	44
12. Experimental setup for seeding experiment	55
13. Schematic of the high finesse interferometer	56
14. Raw data for seeding experiment	57
15. Sorted data for seeding experiment	58
16. Output Stokes energy as a function of pump energy	59
17. Experimental setup for spatial structure experiment	68
18. Theoretical prediction for the spatial structure as a function of detuning	69
19. Real part of the Raman susceptibility	70
20. Normalized Stokes energy as a function of detuning	71
21. Experimental results for the spatial structure	72
22. Normalized Stokes energy as a function of detuning and gain	80
23. Raman linewidth	81
24. Detuning that maximizes Stokes output as a function of gain	82
25. Experimental setup for asymmetric gain experiment	83
26. Stokes output as a function of seed frequency	84
27. Experimental detuning that maximizes the Stokes output as a function of gain	85
D1. The U_0^0 Gauss-Laguerre mode	110
D2. The U_2^0 Gauss-Laguerre mode	111
D3. The U_0^2 Gauss-Laguerre mode	112
D4. The U_2^2 Gauss-Laguerre mode	113
F1. Experimental setup for mode matching	121
F2. Experimental apparatus to align the HFI	122
F3. Video image and oscilloscope trace at various stages of mode matching	123
G1. Raman linewidth as a function of pressure	127

ABSTRACT

A theory is presented for an injection seeded Raman amplifier which includes the total Raman susceptibility. Calculations indicate that the imaginary part of the Raman susceptibility leads to gain and gain guiding while the real part of the Raman susceptibility leads to index guiding. Both the gain and index guiding affect the spatial structure of the amplified Stokes beam. When the input Stokes beam is tuned to the blue (red) side of the Raman resonance, the amplified Stokes beam is focused (defocused) due to the real part of the Raman susceptibility. The calculations also indicate the peak Stokes output from the Raman amplifier occurs when the input Stokes is tuned to the blue side of the Raman resonance. Experimental results are presented that measure the amplified Stokes beam's spatial structure. The results from this experiment confirm the prediction of a narrower (wider) Stokes beam when the input Stokes is tuned to the blue (red) side of the Raman resonance. The narrower amplified Stokes beam when the input Stokes is tuned to the blue side of the Raman resonance results in the amplified Stokes beam experiencing an increased gain. This increased gain that occurs on the blue side of the Raman resonance is confirmed by an experiment.

CHAPTER 1

INTRODUCTION

Raman Scattering

Raman scattering¹⁻³ is an inelastic scattering process in which a photon is scattered off a Raman active medium. Because the scattering process is inelastic, the scattered photon can either deposit some of its energy in the Raman active medium which results in a red shifted scattered photon or extract some energy from the Raman active medium which results in a blue shifted scattered photon. The red shifted scattered photon is often referred to as a Stokes photon while the blue shifted scattered photon is referred to as an antiStokes photon.

A schematic energy level diagram for a typical Raman scattering process is shown in Fig.1. The energy level labeled $|1\rangle$ is the ground state of the Raman active medium, the energy level labeled $|2\rangle$ is usually the first excited electronic state, and the energy level labeled $|3\rangle$ can result from a vibrational or rotational excited state of the Raman active medium. A pump photon with energy $\hbar\omega_p$, where ω_p is the frequency of the

pump photon, is scattered off the Raman active medium leaving the Raman active medium in the excited state $|3\rangle$. The energy of the scattered photon can be found from conservation of energy to be $\hbar\omega_s = \hbar\omega_p - \hbar\omega_{13}$ where $\hbar\omega_{13}$ corresponds to the energy difference between levels $|1\rangle$ and $|3\rangle$ shown in Fig.1 and ω_s is the frequency of the scattered photon. The frequency of the scattered photon has been red shifted and the scattered photon is referred to as a Stokes photon.

Scattering can occur either by spontaneous scattering or stimulated scattering. Spontaneous scattering occurs when just a pump photon is incident on the Raman active medium. A single Stokes photon is created at the frequency ω_s after the scattering event has occurred. Stimulated Raman scattering occurs when both a pump photon at the frequency ω_p and an input Stokes photon at ω_s are incident on the Raman active medium. Two Stokes photons at the frequency ω_s come out after the scattering event. In the case of stimulated Raman scattering, the input Stokes photon is amplified by the scattering event.

A simplified schematic of an experiment which studies stimulated Raman scattering is shown in Fig.2. A high power laser provides a source of pump photons for the stimulated Raman scattering. Input Stokes photons can be generated for example by spontaneous emission or by a tunable laser diode centered at the frequency ω_s . The input Stokes photons are combined at the beam combiner with the pump photons and sent colinearly through a Raman active medium. The amplified Stokes and residual pump are separated by a dispersive element such as a prism.

The Raman active medium used for all the work in this thesis is diatomic hydrogen. The H_2 is contained in a cell at high pressures. The state labeled $|1\rangle$ in Fig.1 is the ground state of the H_2 molecule while the state labeled $|2\rangle$ is the first excited electronic state and is 11.2eV above the ground state. The state labeled $|3\rangle$ is the first excited vibrational state and is 0.51eV above the ground state. The source of pump photons in the experiments to be discussed in this thesis come from a frequency doubled Nd:YAG laser at a wavelength of $\lambda_p=532\text{nm}$ which corresponds to an energy for the pump photon of 2.33eV. The scattered Stokes photons are at a wavelength of $\lambda_s=683\text{nm}$ which corresponds to an energy for the scattered Stokes photon of 1.82eV.

Background

Laser induced Raman scattering was first studied in 1962⁴ and ever since has provided a productive area for research. Raman scattering is used in spectroscopic systems^{3,5} where the frequency shift of the scattered light, which is characteristic of the scattering medium, is used to identify the scatterer. Raman scattering is also used as a way to shift frequencies of lasers by integer multiples of the frequency ω_{13} ^{6,7} (shown in Fig.1). More recently, Raman scattering has been used to study temporal solitons⁸⁻¹⁴. It was found that the Raman solitons occur spontaneously and the origin of this phenomena is a result of quantum fluctuations^{8,14}. The quantum fluctuations or quantum noise were shown to be at the one photon per mode noise limit for a phase insensitive optical amplifier^{15,16}. The noise limit of one photon per mode implies that the quantum noise can

easily be dominated in a Raman amplifier by using an input Stokes signal of only a few photons.

More recently, work has focused on looking at the full three dimensional aspect of the Raman amplifier. The focused nature of the pump beam and transverse variations in the gain are taken into account in a theory which utilizes a nonorthogonal modal basis expansion to describe the amplified Stokes field¹⁷⁻²². The initial nonorthogonal modal theory describes the energy output of the Raman amplifier¹⁹ but fails to correctly predict the spatial structure of the amplified Stokes output. Modifying the wave equation to include the effects of index guiding and using a similar nonorthogonal modal expansion to describe the amplified field correctly predicts the measured spatial structure of the amplified Stokes output²³. Including the effects of index guiding also leads to the unintuitive prediction that the peak Stokes output does not occur when the input Stokes signal is tuned to the Raman resonance but rather occurs when the input Stokes signal is tuned to the blue side of the Raman resonance²⁴. Investigating the index guiding effects in a Raman amplifier is the main thrust of this thesis.

Gain and Index Guiding

Gain^{19,20,25} and index^{23,24,26} guiding are two effects which influence the spatial structure of the amplified Stokes beam as it grows in a Raman amplifier. In fact, gain and index guiding will occur whenever a gain profile that is nonuniform in the transverse

direction is present. The work done in this thesis with Raman amplifiers will carry over into many other types of optical amplifiers.

Gain guiding, as the name implies, is related to the gain of an amplifier. The origin of the gain in the Raman amplifier can be traced back to the imaginary part of the Raman susceptibility¹. Most theories which have described Raman amplifiers to this point have only included the imaginary term of the Raman susceptibility⁸⁻²². However, the Kramers-Kronig relationship¹ tells us that if we have an imaginary part of the Raman susceptibility then we must also have a real part of the Raman susceptibility. The real part of the Raman susceptibility affects the index of refraction¹ that the amplified Stokes beam experiences and leads to index guiding. Because the real and imaginary parts of the Raman susceptibility are intertwined by the Kramers-Kronig relationships, gain and index guiding are intertwined and their effects must be studied together.

Gain guiding affects the spatial structure of the amplified Stokes beam as follows. The gain profile in a Raman amplifier is proportional to the pump laser intensity and has a gaussian profile. The input Stokes grows faster at the center of the gain profile where the gain is larger than at the wings. Because the center of the Stokes beam grows more rapidly than the wings, the amplified Stokes beam narrows.

Index guiding also affects the structure of the Stokes beam and acts as follows. The real part of the Raman susceptibility leads to an index of refraction which has a nonuniform transverse profile. A lens can be modeled by a nonuniform transverse index

of refraction. Therefore, we can say that the real part of the Raman susceptibility creates an effective lens which will change the spatial structure of the amplified Stokes beam.

To understand the spatial structure of the amplified Stokes beam, the Raman susceptibility must be included in the wave equation that describes the Raman amplifier. No noise term will be included in this wave equation since we are modeling an injection seeded Raman amplifier where the input Stokes signal is large enough to dominate the effects of quantum noise.

The wave equation is solved in chapter 2 by two different methods. The first method involves expanding the amplified Stokes field over the Gauss-Laguerre basis^{27,28}. The Gauss-Laguerre basis turns out to be a nice basis to work with because the input Stokes field is a focused gaussian and can be described by only the lowest order Gauss-Laguerre mode. The input mode is coupled to several modes in the Raman amplifier via the Raman gain and this allows the output of the Raman amplifier to have a different spatial structure than the input Stokes signal. The output of the Raman amplifier however is described by many modes and this makes the Gauss-Laguerre basis awkward for describing the output of the Raman amplifier. The second method of solution which will also be presented in chapter 2 involves expanding the amplified Stokes field over a nonorthogonal modal basis¹⁷⁻²². The nonorthogonal modal basis is a natural modal basis for describing the output of the Raman amplifier. In the high gain limit, the amplified output Stokes field can be described by a single nonorthogonal mode¹⁹. However, the

input to the Raman amplifier which is a focused gaussian must now be expanded over the more complicated nonorthogonal modes.

The numerical results from solving the wave equation are presented in chapter 3. The effects of gain and index guiding on the spatial structure including the phasefronts are studied in this chapter. Surprisingly, the numerical results indicate that tuning the input Stokes signal to the blue side of Raman resonance can be used to increase the output of the Raman amplifier. A brief discussion on improving the performance of the Raman amplifier by modifying the phasefronts of the input Stokes beam to better overlap the phasefronts supported by the Raman amplifier is presented.

Three experiments, presented in chapters 4,5,and 6, use a tunable laser diode as a source of input Stokes photons. The first experiment, presented in chapter 4, shows that the input Stokes signal can effectively couple to a Raman amplifier. This experiment will show that only a few photons in the input Stokes are needed to dominate the quantum noise (spontaneous emission). The second experiment, presented in chapter 5, involves imaging the amplified Stokes beam at the exit of the Raman amplifier. The experimental results are not explained by previous work that only considered gain guiding but rather are in agreement with the predictions of gain and index guiding. Finally, the last experiment, to be considered in chapter 6, examines the Stokes output energy as a function of detuning. It is found that the peak Stokes output occurs when the input Stokes signal is tuned to the blue side of the Raman resonance in agreement with the predictions of the theory which includes both gain and index guiding.

Chapter 7 contains concluding remarks on how index guiding affects the growth of the amplified Stokes beam in a Raman amplifier. Possible future experiments are also mentioned.

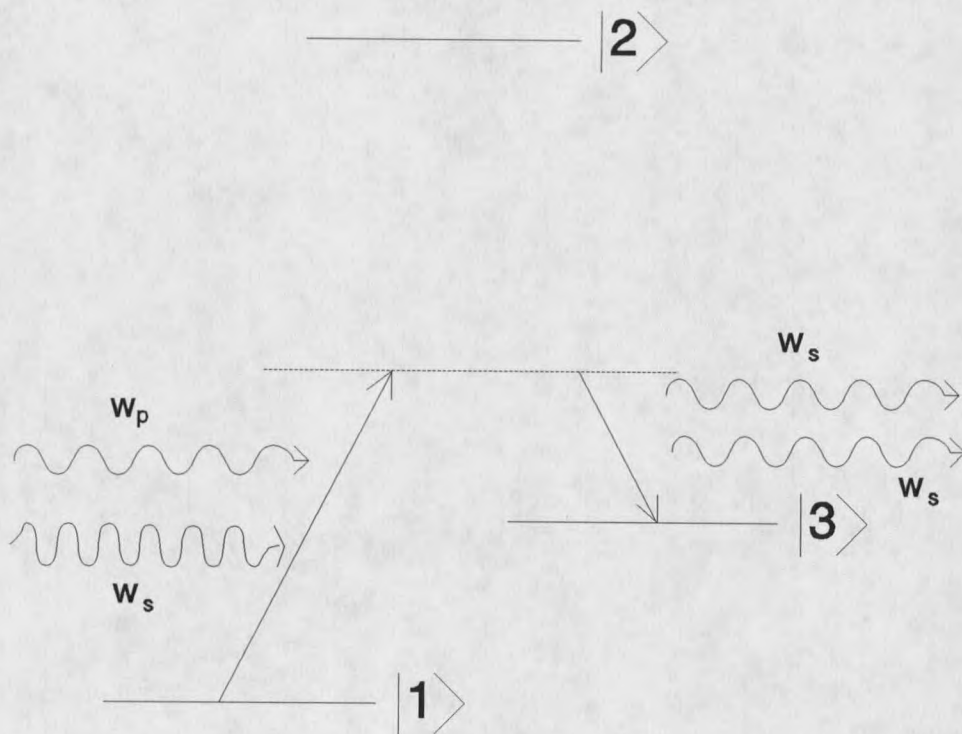


Figure 1 Schematic energy level diagram for Raman scattering

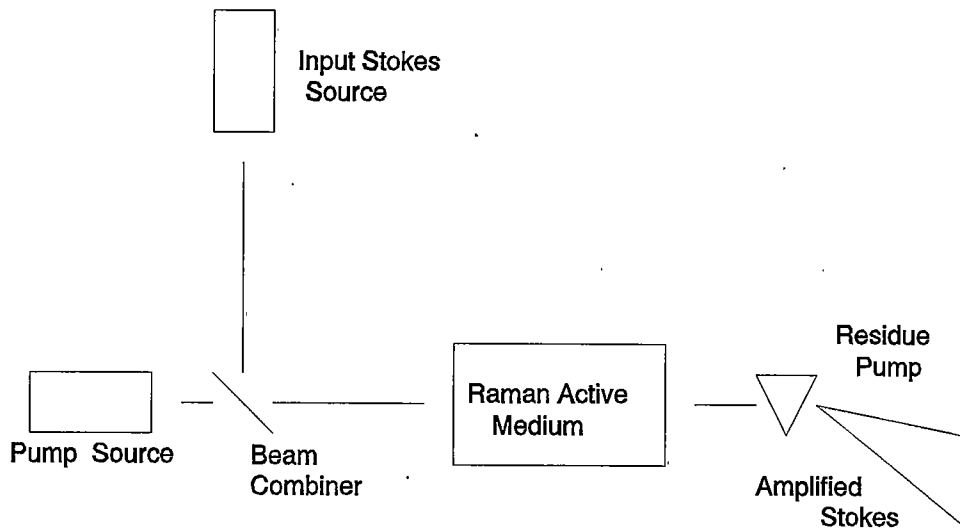


Figure 2 Simplified experimental setup to study stimulated Raman scattering

CHAPTER 2

THE WAVE EQUATION AND METHOD OF SOLUTION

Introduction

The mathematical formalism developed in this chapter allows us to numerically look at solutions to the wave equation that describes the Raman amplifier. First, the wave equation that describes the Raman amplifier is presented. The nonlinear Raman susceptibility is presented next. The nonlinear Raman susceptibility results from the H_2 molecule being driven by the beating of the Stokes and pump fields during the scattering process. Next, some limiting case solutions to the wave equation are studied. These solutions aid in understanding how the real and imaginary parts of the nonlinear Raman susceptibility affect the amplified Stokes field. Finally, two different methods of solution to the wave equation are presented which depend on modal expansions of the Stokes field. As mentioned in the first chapter, expanding the Stokes field over a Gauss-Laguerre basis allows one to describe a gaussian input in terms of a single mode. Also, more complicated inputs to the Raman amplifier are more easily described in terms of the

orthogonal Gauss-Laguerre basis than the nonorthogonal modal basis. While the Gauss-Laguerre basis is useful for describing the input into the Raman amplifier, the nonorthogonal modal basis is useful for describing the Raman amplifier output because only one nonorthogonal mode is needed to describe the amplifier output in the high gain limit. Since the choice of basis is not obvious, the solution to the wave equation using both a Gauss-Laguerre basis and a nonorthogonal basis is presented later in this chapter.

Wave Equation

In the work done in this thesis, we are interested in describing the Raman amplifier in the steady state paraxial limit. The three dimensional wave equation that describes the Raman amplifier is written

$$\nabla_T^2 E_s(z, r_T) - 2ik_s \frac{\partial}{\partial z} E_s(z, r_T) = -\frac{4\pi\omega_s^2}{c^2} \chi_{NL} |E_p|^2 E_s(z, r_T) \quad 2.1$$

where $\nabla_T^2 = \frac{\partial^2}{\partial x^2} + \frac{\partial^2}{\partial y^2}$ is the transverse laplacian, $E_s(z, r_T)$ is the slowly varying Stokes field, k_s is the Stokes wavevector, ω_s is the frequency of the Stokes field, c is the speed of light, χ_{NL} is the nonlinear Raman susceptibility and E_p is the pump field. The wave equation is derived in appendix A. The fully transient equations that describe the Raman amplifier are presented in appendix B along with a link to the above wave equation in the steady state limit.

The Nonlinear Raman Susceptibility

The nonlinear Raman susceptibility, χ_{NL} , is responsible for the Raman gain, gain guiding effects, and index guiding effects. The nonlinear Raman susceptibility in vibrational Raman scattering from diatomic hydrogen results from an induced dipole moment of the H_2 molecule due to the beating of the pump and Stokes field¹. In this case we can let the vibrational frequency, ω_v , of the H_2 molecule define the Raman resonance. In appendix C the H_2 molecule is modeled as a damped driven harmonic oscillator with a resonant frequency ω_v . This model yields a nonlinear Raman susceptibility that can be written

$$\chi_{NL} = \frac{N \left(\frac{\partial \alpha}{\partial X} \Big|_0 \right)^2}{16m\omega_v} \left(\frac{\Delta}{\Delta^2 + \frac{\gamma^2}{4}} + i \frac{\frac{\gamma}{2}}{\Delta^2 + \frac{\gamma^2}{4}} \right) \quad 2.2$$

where N is the number density of H_2 molecules, α is the molecular polarization, m is the reduced mass of the H_2 molecule, $\Delta = \omega_v - (\omega_p - \omega_s)$ is the detuning away from the Raman resonance, and γ is related to the collisional dephasing rate, Γ , by the relationship $\Gamma = \gamma / 2$.

A definition is made for the Raman susceptibility χ_R such that

$$\chi_R = \chi_{NL} |E_p|^2 \quad 2.3$$

One can write the Raman susceptibility from Eq.2.2 and Eq.2.3 as

$$\chi_R = \frac{N \left(\frac{\partial \alpha}{\partial X} \Big|_0 \right)^2}{16m\omega_v} \left(\frac{\Delta |E_p|^2}{\Delta^2 + \frac{\gamma^2}{4}} + i \frac{\frac{\gamma}{2} |E_p|^2}{\Delta^2 + \frac{\gamma^2}{4}} \right) \quad 2.4$$

Approximate Solutions To The Wave Equation

Before the solution to the wave equation, Eq.2.1, is presented in its full detail, some approximations are made to simplify the wave equation. Two objectives are reached in studying the simplified wave equation. The first objective is to cast the Raman susceptibility in terms of the parameters that are used in the literature such as k_s , the Stokes wavevector, $g(z, r_T)$, the gain profile, Δ , the detuning, and Γ , the collisional dephasing rate. The second is to obtain an understanding of how the Raman susceptibility influences the Stokes field.

The Raman susceptibility for a molecule can be written as $\chi_R = \chi' - i\chi''$ where the real and imaginary parts of the Raman susceptibility are defined in Eq.2.4. The constants in Eq.2.4 are determined by requiring that the Stokes growth predicted by the wave equation (Eq.2.1) be equal to the Stokes growth given in Refs.[29,30]. The results in Refs.[29,30] were derived under the assumption that no index guiding occurred

($\chi' = 0$) and diffraction of the Stokes field was negligible ($\nabla_T^2 E_s(z, r_T) \approx 0$). With these approximations the wave equation (Eq.2.1) can be written

$$\frac{\partial E_s(z)}{\partial z} = -\frac{2\pi\omega_s^2}{k_s c^2} \chi'' E_s(z) \quad 2.5$$

which has

$$E_s(z) = E_s(0) e^{-\frac{2\pi\omega_s^2}{k_s c^2} \chi'' z} \quad 2.6$$

as the solution for the field. Squaring the field leads to the Stokes intensity and the Stokes intensity is written

$$I_s(z) = I_s(0) e^{-\frac{4\pi\omega_s^2}{k_s c^2} \chi'' z} \quad 2.7$$

On the other hand, Refs.[29,30] show that the Stokes intensity is

$$I_s(z) \propto e^{\frac{g^2 z}{\Delta^2 + \Gamma^2}} \quad 2.8$$

comparing Eqs.2.7 and 2.8 we obtain $-\frac{4\pi\omega_s^2}{k_s c^2} \chi'' = g \frac{\Gamma^2}{\Delta^2 + \Gamma^2}$. Combining this result

with Eq.2.4 allows us to write the Raman susceptibility as

$$\chi_R = \frac{k_s c^2}{4\pi\omega_s^2} g(z, r_T) \left(\frac{\Delta\Gamma}{\Delta^2 + \Gamma^2} + i \frac{\Gamma^2}{\Delta^2 + \Gamma^2} \right) \quad 2.9$$

where the gain $g \rightarrow g(z, r_T)$ has been included to allow for the spatial variation of the gain profile.

Some insight into the effects of χ' and χ'' can be gleaned by solving the wave equation under the assumption that the diffraction of the Stokes field is negligible, ($\nabla_T^2 E_s(z, r_T) \approx 0$). The wave equation is written

$$\frac{\partial E_s(z, r_T)}{\partial z} = \frac{2\pi\omega_s^2}{ik_s c^2} (\chi' - i\chi'') E_s(z, r_T) \quad 2.10$$

The solution to Eq.2.10 is a simple exponential

$$E_s(z, r_T) = E_s(0, r_T) e^{-\frac{2\pi\omega_s^2}{k_s c^2} \chi'' z - i \frac{2\pi\omega_s^2}{k_s c^2} \chi' z} \quad 2.11$$

where $E_s(0,r_T)$ is the input Stokes field. From Eq.2.11, the imaginary part of the Raman susceptibility, χ'' , leads to gain (absorption) if $\chi'' < 0$ ($\chi'' > 0$). Also from Eq.2.11 the real part of the Raman susceptibility, χ' , leads to a phase shift. The transverse variation in the real part of the Raman susceptibility which results from the gain profile results in a phase shift that varies in the transverse direction. This phase shift can be thought of as caused by an index of refraction and is analogous to a phase shift resulting from a field passing through a lens. The real part of the Raman susceptibility can be thought of as creating an effective lens that can focus or defocus the Stokes beam and this leads to index guiding.

Solution To The Wave Equation

The wave equation is solved using a modal expansion of the Stokes field. The question of which basis to use for the expansion of the Stokes field is a difficult one. Ideally, the Stokes field would be described throughout the Raman amplifier by a single mode of the basis chosen. A Gauss-Laguerre basis^{24,27} allows the input to be written as a single mode. The susceptibility couples this single input mode to several higher order modes with the same cylindrical symmetry as the gain but with different radial profiles. Coupling a single input mode to several modes at the exit of the Raman amplifier allows for the changes in the spatial structure of the amplified Stokes. A second more complicated basis that can be used to describe the Stokes field in a Raman amplifier is the nonorthogonal modal basis¹⁷⁻²². This basis has the nice property that only the lowest

order nonorthogonal mode is needed to describe the output of the Raman amplifier¹⁹. However, the gaussian input signal must be expanded over the more complicated nonorthogonal basis. Solutions to the wave equation using both a Gauss-Laguerre and nonorthogonal basis are presented in this section.

The Gauss-Laguerre Basis

Using the wave equation (Eq.2.1) and the Raman susceptibility (Eq.2.4), the Raman amplifier is described by

$$\nabla_T^2 E_s(z, r_T) - 2ik_s \frac{\partial E_s(z, r_T)}{\partial z} + ik_s g(z, r_T) \left(\frac{\Gamma^2}{\Delta^2 + \Gamma^2} - i \frac{\Gamma \Delta}{\Delta^2 + \Gamma^2} \right) E_s(z, r_T) = 0 \quad 2.12$$

The wave equation includes the real and imaginary parts of the Raman susceptibility with Δ , the detuning from the Raman resonance and Γ , the Raman linewidth³¹, explicitly included in the wave equation. The assumption that the spontaneous emission is negligible has been used and therefore no terms are needed in Eq.2.12 to account for the spontaneous emission. The validation of this assumption will be discussed more in chapter 4.

The focused nature of the pump beam is taken into account in the gain profile. In this work we will consider a focused gaussian gain profile^{19,24,27,32}

$$g(z, r) = \frac{4G}{k_g \omega_g^2(z)} e^{-2r^2/\omega_g^2(z)} \quad 2.13$$

where G is related to the plane wave gain coefficient³³, k_g is the pump laser wavevector, the gaussian beam waist is $\omega_g(z) = \omega_g(0)\sqrt{1 + (z/z_0)^2}$, r is the magnitude of the transverse radius vector r_T , and z_0 is the Rayleigh range of the focused gaussian profile. The gain profile has rotational symmetry about the z axis and, therefore, it will be convenient to work in cylindrical coordinates.

The wave equation is similar to a wave equation solved by Perry et.al.²⁷ and the details of their solution are presented in Ref.[27]. A brief outline is presented here with the changes needed to account for χ' and the consequent index guiding effects. The Stokes field is expanded over a complete set of orthonormal Gauss-Laguerre modes $U_p^l(z, r_T)$. The Gauss-Laguerre modes are the solution to Eq.2.1 when the Raman susceptibility is set equal to zero. These modes solve the wave equation for free space propagation and are referred to as the modes of free space. The Gauss-Laguerre modes are defined in appendix D along with plots of some lower order modes.

The Stokes field is written as an expansion of the Gauss-Laguerre modes as

$$E_s(z, r_T) = \sum_{p,l} V_p^l(z) U_p^l(z, r_T) \quad 2.14$$

where $V_p^l(z)$ are the field expansion coefficients. Substituting Eq.2.14 into Eq.2.12 and using the orthonormal properties of the Gauss-Laguerre modes yields the following set of linear coupled differential equations in z for the field expansion coefficients

$$\frac{dV_{p'}^{l'}}{dz} = \sum_{p,l} G_{p',p}^{l',l}(z) V_p^l(z) \quad 2.15$$

where

$$G_{p',p}^{l',l} = \frac{1}{2} \left(\frac{\Gamma^2}{\Delta^2 + \Gamma^2} - i \frac{\Gamma\Delta}{\Delta^2 + \Gamma^2} \right) \int_0^{2\pi} d\varphi \int_0^\infty r dr \left[U_{p'}^{l'*}(z, r_T) g(z, r_T) U_p^l(z, r_T) \right] \quad 2.16$$

Substituting the focused gaussian gain profile from Eq.2.13 and noting that the integration over φ results in non zero terms only when $l = l'$, the following expression for $G_{p',p}^{l',l}$ is obtained

$$G_{p',p}^{l',l} = G \frac{2\mu}{\omega_s^2(z) k_g} \left(\frac{\Gamma^2}{\Delta^2 + \Gamma^2} - i \frac{\Gamma\Delta}{\Delta^2 + \Gamma^2} \right) e^{-2i(p'-p)\tan^{-1}(z/z_0)} Q_{p',p}^l(\mu) \quad 2.17$$

where the parameter $\mu = \lambda_p / (\lambda_p + \lambda_s)$ is defined as the mode filling factor with

λ_p (λ_s) the pump (Stokes) wavelength and $Q_{p',p}^l(\mu)$ is a polynomial in powers of μ and

is defined in appendix E. The fact that only nonzero terms result from $l = l'$ can be argued on the physical grounds that the modes which describe the Stokes field must have the same angular dependence as the gain.

The important substitution of variable

$$\theta = \tan^{-1}(z / z_0) \quad 2.18$$

is made to fold out the focusing nature of the problem. The equation for the field expansion coefficients becomes

$$\frac{dV_{p'}^l(\theta)}{d\theta} = \sum_p M_{p',p}^l(\theta) V_p^l(\theta) \quad 2.19$$

where

$$M_{p',p}^l(\theta) = \mu G \left(\frac{\Gamma^2}{\Delta^2 + \Gamma^2} - i \frac{\Gamma \Delta}{\Delta^2 + \Gamma^2} \right) Q_{p',p}^l(\mu) e^{-2i(p'-p)\theta} \quad 2.20$$

The solution for the field expansion coefficients is

$$V_{p'}^l(\theta) = \sum_p A_{p',p}^l(\mu, G; \theta, \theta_m) V_p^l(\theta_m) \quad 2.21$$

where the matrix elements $A_{p',p}^l(\mu, G; \theta, \theta_{in})$ are defined in appendix E, θ_{in} defines the input of the Raman amplifier, and θ defines the location in the Raman amplifier. The field expansion coefficients, $V_p^l(\theta_m)$, are used to represent the input Stokes signal. When the Raman amplifier is seeded with a gaussian input signal, only the $p=l=0$ element of $V_p^l(\theta_m)$ will be nonzero and the input Stokes power will be proportional to $|V_0^0(\theta_m)|^2$. In this case the sum in Eq.2.21 will drop out.

Because only the $p=l=0$ element is needed to describe the input mode, the Gauss-Laguerre modes are a convenient choice for the Stokes field expansion. However, the coupling element $G_{p',p}^l$ couples this single input mode to several output modes for each individual l . The fact that many modes can couple together allows the amplified Stokes beam to have a different combination of spatial modes than the input Stokes signal and hence the amplified Stokes can have a significantly different spatial structure than the input Stokes signal. Notice however, that since the gain does not couple the input field to modes with different angular indices ("l" values), it is necessary to solve the above matrix equation for $l=0$ only.

The Nonorthogonal Basis

The wave equation presented in Eq.2.12 and the gain profile presented in Eq.2.13 are again the starting point. However, instead of expanding the Stokes field over the

Gauss-Laguerre basis, it is now expanded over a nonorthogonal basis¹⁷⁻²². The solution presented here is very similar to the solution presented in Ref.[19] and only a brief outline of the solution is presented here to show the changes needed to include the real part of the Raman susceptibility which allows for index guiding effects. The Stokes field is written as an expansion over the nonorthogonal modes as

$$E_s(z, r_T) = \sum_{n,l} a_n^l(z) \Phi_n^l(z, r_T) \quad 2.22$$

where $a_n^l(z)$ is the amplitude of the nonorthogonal mode $\Phi_n^l(z, r_T)$. The nonorthogonal modes are required to satisfy the eigenvalue equation

$$\left(\nabla_T^2 - 2ik_s \frac{\partial}{\partial z} + ik_s g(z, r_T) \left(\frac{\Gamma^2}{\Delta^2 + \Gamma^2} - i \frac{\Gamma \Delta}{\Delta^2 + \Gamma^2} \right) \right) \Phi_n^l(z, r_T) = \lambda_n^l \frac{4ik_s}{k_g \omega_g^2(z)} \Phi_n^l(z, r_T) \quad 2.23$$

The nonorthogonal modes are written as a summation over the free space Gauss-Laguerre modes. The summation in this case is only over the radial indices of the Gauss-Laguerre modes because the gain profile has rotational symmetry and only the $l=0$ angular indice has the proper rotational symmetry to match the gain profile. The nonorthogonal modes are written

$$\Phi_n^l(z, r_T) = \sum_p b_{n,p}^l U_p^l(z, r_T) \quad 2.24$$

where $b_{n,p}^l$ are the free space mode coefficients. Making the change of variable

$\theta = \tan^{-1}(z / z_0)$ and using Eq.2.23 and Eq.2.24, the equation of motion for the free

space mode coefficients becomes

$$\frac{\partial b_{n,p'}^l}{\partial \theta} - \sum_p b_{n,p}^l e^{-2ip'\theta} K_{p',p}^l(\mu) e^{2ip\theta} = \lambda_n^l b_{n,p'}^l \quad 2.25$$

where

$$K_{p',p}^l(\mu) = \frac{\mu G z_0}{\pi \omega_g^2(0)} \left(\frac{\Gamma^2}{\Delta^2 + \Gamma^2} - i \frac{\Gamma \Delta}{\Delta^2 + \Gamma^2} \right) Q_{p',p}^l(\mu) \quad 2.26$$

where $Q_{p',p}^l(\mu)$ is defined in appendix E.

Equation 2.25 can be transformed into an operator equation by defining the vector

b_n^l which represents the free space mode coefficients $\{b_{n,p}^l\}$ and writing $K_{p',p}^l$ as a matrix

K^l . The operator equation becomes

$$\left[\frac{\partial}{\partial \theta} - e^{-iH\theta} K^l e^{iH\theta} - \lambda_n^l \right] b_n^l = 0 \quad 2.27$$

where $H'_{p',p} = 2p\delta_{p',p}$. The solution to Eq.2.27 is

$$b'_n = e^{-iH\theta} \lambda'_n \quad 2.28$$

where λ'_n satisfy the eigenvalue equation

$$(K' + iH)\chi'_n = \lambda'_n \chi'_n \quad 2.29$$

The details of the solution to Eq. 2.29 are presented in Ref[19]. Finally, the nonorthogonal mode can be written

$$\Phi'_n(z, r_T) = \sum_p e^{-2ip\theta} U'_p(z, r_T) \lambda'_{n,p} \quad 2.30$$

The Stokes field is written as a superposition of the nonorthogonal modes. The nonorthogonal modes have been calculated above. Next, the expansion coefficients (a'_n) need to be calculated. Substituting the field expansion (Eq.2.22) into the wave equation leads to the equation

$$\sum_n -2ik_s \left(\frac{\partial a_n'}{\partial z} + \lambda_n' \frac{2}{k_g \omega_g^2(z)} \right) = 0 \quad 2.31$$

The solution to Eq.2.31 is

$$a_n'(z) = a_n'(0) e^{-\frac{2}{k_g \omega_g^2(z)} \lambda_n'} \quad 2.32$$

where $a_n'(0)$ is the projection of the input Stokes signal on the Φ_n' nonorthogonal mode.

The amplified Stokes field is finally constructed from Eqs.2.22, 2.30, and 2.32.

Armed with the solution to the wave equation we are now ready to study the effects of index guiding in a Raman amplifier.

CHAPTER 3

MODE STRUCTURE OF THE AMPLIFIED STOKES FIELD

Introduction

The effects of gain and index guiding on the amplified Stokes beam in a Raman amplifier are numerically studied in this chapter. The wave equation presented in chapter two is solved using both the nonorthogonal modal expansion and the Gauss-Laguerre modal expansion. These two different methods of solution yield the same results, as expected.

The wave equation was solved in chapter two for the limiting case of no diffraction, and we saw how the imaginary part of the Raman susceptibility led to gain and the real part of the Raman susceptibility led to a phase shift that is associated with an index of refraction. In the next section, physical arguments are made to describe how the gain leads to gain guiding and how the index of refraction leads to index guiding. Next, the phasefronts of the amplified Stokes field are studied along with the spatial structure of

the amplified Stokes field. Finally, some comments about enhanced coupling into a Raman amplifier are presented in terms of the mode structure and detuning.

Physical Arguments For Gain And Index Guiding

Gain guiding works to narrow the amplified Stokes beam in the following way. For a focused gaussian pump beam, the center of the gain profile, which is proportional to the pump intensity, amplifies the center of the signal more than the wings because the gain is larger near the center of the gain profile. Because the center of the amplified Stokes grows more than the wings, the amplified Stokes beam narrows.

Figure 3 is a graphic representation of gain guiding. The dot-dashed line represents a gaussian gain profile with a maximum gain of 2.5. The dashed line is the input signal and has a maximum intensity of 1 and the full width at half maximum (FWHM) is shown. The amplified field is found by multiplying the input signal times the exponential of the gain (exponential growth). The amplified field is shown as the solid line in Fig.3 and the FWHM is labeled. Note that the FWHM of the amplified field is narrower than the FWHM of the input signal. The exponential growth used to generate the amplified field for Fig.3 is a good model for the amplification in a Raman amplifier.

A review of a focusing lens will help in the physical explanation of how index guiding works. Figure 4 shows a plane wave impinging on a lens from the left. The optical path length which is a product of the length which the light travels multiplied by the index of refraction of the material through which the light travels is larger at the

center of the lens than at the wings of the lens. The phasefront is retarded more near the center of the lens because the light travels through a larger optical path length than the wings.. This is why the phasefront appears curved after the lens. As the beam propagates further, diffraction causes the phasefront to change as shown in Fig.4.

The phase shift of the amplified Stokes field in a Raman amplifier is proportional to the real part of the Raman susceptibility as was seen in Eq.2.16. The real part of the Raman susceptibility is written $\chi' = g(z, r_T) \left(\frac{\Gamma \Delta}{\Delta^2 + \Gamma^2} \right)$. The gain profile is proportional to the pump laser intensity and is a gaussian. When the input Stokes is detuned to the blue side of the Raman resonance so that $\Delta \neq 0$, the real part of the Raman susceptibility causes the Stokes field to see an optical path length similar to that shown in Fig.4. Hence, when the Stokes seed is detuned to the blue side of the Raman resonance, the amplified field experiences an effective lens caused by the phase shift related to the real part of the Raman susceptibility. The ability of the Raman medium to focus the Stokes beam is referred to as index guiding.

Mode Structure Of The Amplified Stokes Field

The phasefronts and spatial structure of the lowest order nonorthogonal mode and gaussian input Stokes signal are studied in this section for two cases. The first case occurs when the input signal is tuned exactly to the Raman resonance, $\Delta = 0$, and therefore the Raman susceptibility is purely imaginary which leads to gain without any index guiding effects. This case will allow us to understand how gain guiding effects the

nonorthogonal mode. In the second case, $\Delta \neq 0$, and the Raman susceptibility contains both an imaginary and a real term. In this case the Raman susceptibility leads to an index of refraction which gives rise to index guiding. Thus, in the second case both index and gain guiding are considered.

Unless otherwise noted, the following parameters which describe the Raman amplifier are used in the calculations for this chapter. For parameters that are typical of Raman amplifier experiments, the difference in the phasefronts would be difficult to show in the figures. Therefore the waist and wavelengths were chosen so that the differences between the phasefronts can easily be seen in the figures. This makes the physical explanation of the mode structure and coupling easier to understand. The Rayleigh range was set at $\sqrt{2}$ cm for both the pump and input Stokes signal. A gain of $G=3$ and a pump beam waist of $\omega_g(0) = 1$ cm were used. The Raman linewidth was set at 3000MHz and the detuning used was $\Delta = 0$ MHz for the on resonance case and $\Delta = \pm 300$ MHz for the off resonance cases. The entrance to the Raman amplifier was at $z/z_{0g} = -2$.

Figure 5 shows the phasefronts for case 1 in which $\Delta = 0$. The solid line shows the phasefronts for the lowest order nonorthogonal mode while the dashed line shows the phasefronts for the gaussian input Stokes mode. The phasefronts are plotted at various locations in the cell defined by z/z_{0g} with the gaussian input signal mode focusing at $z/z_{0g}=0$. For $z/z_{0g}<0$ notice that the curvature of the phasefronts indicate that input signal is focusing while for $z/z_{0g}>0$, the curvature of the phasefronts indicates that the input

signal is diffracting. This is not surprising since the input Stokes signal is a focused gaussian. However, the phasefronts of the nonorthogonal mode are much more complicated and very different than the gaussian input Stokes signal. The phasefronts for case 1 result from competition between gain guiding and diffraction, as discussed below. Notice that the phasefronts of the nonorthogonal mode and gaussian input Stokes signal are poorly matched. This indicates that the Raman amplifier is not being used efficiently^{30,35}.

Gain guiding has the effect of narrowing the Stokes beam as it grows in the Raman amplifier. However, as the Stokes beam becomes narrower it wants to diffract faster. The competition between gain narrowing and diffraction cause the nonorthogonal mode to have phasefronts which are swept back from the input signal gaussian mode indicating a higher rate of diffraction for the nonorthogonal mode which is compensated by the gain narrowing.

Figure 6 shows the spatial structure of both the nonorthogonal mode (solid line) and the gaussian input signal mode (dashed line). The nonorthogonal mode is narrower than the gaussian mode because of gain guiding. It is interesting to note that this result holds throughout the Raman amplifier which may seem surprising because we would expect the narrower nonorthogonal mode to diffract faster than the gaussian mode. The nonorthogonal mode stays narrower because gain guiding can compensate for the diffraction.

Figure 7 shows the index effect when the input Stokes signal is detuned to the blue side of the Raman resonance. As before, the dashed line is the phasefront of the gaussian input Stokes signal and the solid line is the phasefront of the nonorthogonal mode when the detuning is set equal to zero. The dot-dashed line is the phasefront of the nonorthogonal mode when the input signal is detuned to the blue side of the Raman resonance. When the input Stokes signal is detuned to the blue side of the Raman resonance, the index guiding effect changes the phasefront much like a focusing lens. The phasefronts are swept back less when the input Stokes signal is tuned to the blue side of the Raman resonance than when $\Delta = 0$ indicating focusing is occurring. The fact that the index of refraction is trying to guide the Stokes beam gives rise to the term index guiding.

Figure 8 shows the index effect when the input Stokes signal is tuned to the red side of the Raman resonance. The dashed and solid lines are the same as in Fig.7. The dot-dashed line is the phasefront when the input Stokes signal is detuned to the red side of the Raman resonance. The phasefronts on the red side of the resonance are swept back more than when $\Delta = 0$ indicating defocusing is occurring.

The spatial structure of the nonorthogonal mode at $z/z_{0g}=0$ is shown in Fig.9. The dashed and solid lines are the same as in Fig.6 and are shown again for reference. The dot-dashed line shows the intensity profile of the amplified Stokes when the input Stokes signal is detuned to the blue side of the Raman resonance. The dotted line is the intensity profile when the input signal is detuned to the red side of the Raman resonance. When

the input Stokes signal is detuned to the blue (red) side of the Raman resonance the Stokes profile is narrower (wider) than when the input Stokes signal is tuned to the Raman resonance and these results are consistent with the phasefront picture. The use of index guiding to enhance the output of the Raman amplifier is discussed in the next section.

Enhanced Performance of a Raman Amplifier

Efficient coupling of an input signal into an optical amplifier requires that the input signal mode strongly overlap the dominant amplifier mode which has the highest growth rate^{19,30,35}. When the structure of the input signal mode, including the phasefronts, exactly matches the dominant amplifier mode, all of the input signal is available to gain at the highest growth rate. However, if the pump wavelength is different than the signal wavelength or nonlinear effects are occurring such as gain and index guiding in the optical amplifier, it may not be clear how, or even if, the input signal mode can exactly overlap the dominant amplifier mode. If, for example, the phasefronts of the input signal mode and dominant amplifier mode are not matched, interference effects can lower the coupling between these two modes thus diminishing the amplifier performance. Manipulating the structure of the input signal mode to match the amplifier mode can increase the output of the amplifier by forcing the input signal to overlap the dominant amplifier mode.

The overlap of the phasefronts of the gaussian input signal mode and lowest order nonorthogonal mode is poor as seen in Figs.5,7,and 8 when the input mode and lowest order nonorthogonal mode focus at the same location with the same Rayleigh range. By changing the position of focus and Rayleigh range of the input Stokes signal, we can force the phasefronts to better overlap the lowest order nonorthogonal mode and hence enhance the input coupling of the Raman amplifier.

Figure 10 shows that by changing the location of focus and Rayleigh range of the input signal mode, its phasefronts can better overlap the lowest order nonorthogonal mode. The solid lines are the nonorthogonal modes phasefronts whose shape is determined by the Rayleigh range and power of the pump laser. We consider these phasefronts to be fixed and show that by varying the characteristics of the input Stokes signal can enhance coupling into the amplifier. The dashed lines are the phasefronts of the input signal mode with a Rayleigh range and location of focus the same as the pump. The dotted lines are the phasefronts for an input signal mode with a Rayleigh range of one half that of the pump and the focus shifted towards the front of the Raman amplifier. Notice that the dotted lines and solid lines match much better than the solid lines and dashed lines. This indicates that the input signal mode with the shorter Rayleigh range and shifted focus will better overlap the lowest order nonorthogonal mode and thus improve the performance of the Raman amplifier.

Figure 11 summerizes a more detailed study of how the shift in location of the focus can affect the output of the Raman amplifier. The dashed line shows the output of

the Raman amplifier as a function of the focal position of the input Stokes signal when the pump and input signal have the same Rayleigh range. The output Stokes energy has been normalized so that when the pump and input Stokes signal have the same Rayleigh range the output Stokes energy is unity. When $z_{0s}=z_{0g}$ the output of the Stokes signal is enhanced 5% by shifting the focus of the input signal towards the front of the Raman amplifier by approximately one half a Rayleigh range. The solid line is the output Stokes energy as a function of the relative focus when the Rayleigh range of the input signal is one half that of the pump. When the focus of the input Stokes signal is shifted towards the entrance of the Raman amplifier by approximately one Rayleigh range the output Stokes is increased by over 20%. The output Stokes is further increased when the input Stokes signal is tuned to the blue side of the Raman resonance. The dot-dashed line is the same as the solid line except that the input Stokes has been detuned to the blue side of the Raman resonance. The output is enhanced by over 40% when the input signal has been modified and tuned to the blue side of the Raman resonance. This implies that by carefully setting up an optical amplifier, the output can be significantly increased without changing the pump power.

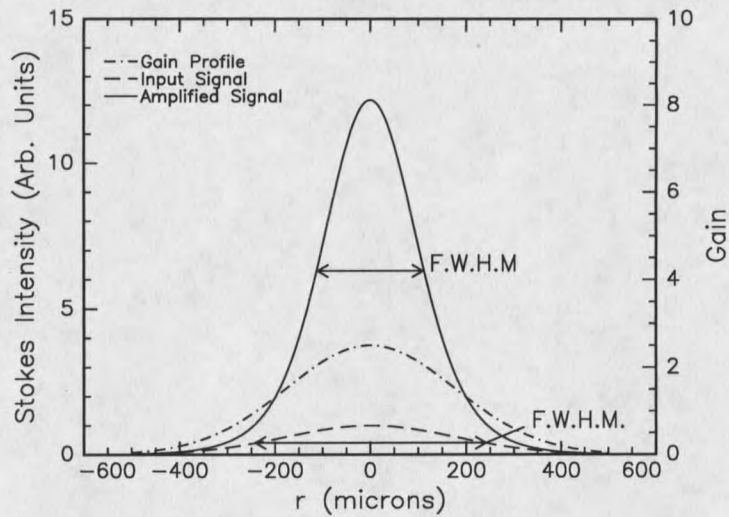


Figure 3 Plot to show how gain guiding works. The dot-dashed line represents the gaussian gain profile, the dashed line represents the transverse profile of the input beam and the solid line represents the transverse profile of the amplified beam.

